ANALYTICAL MODELING AND NUMERICAL SOLUTION OF A SIMPLE SOLAR STILL

De Paula A. C. O.*, Ismail K. A. R. and Salinas C. T.
*Author for correspondence
Department of Energy,
Faculty of Mechanical Engineering
State University of Campinas,
Rua Mendeleyev, 200, Cidade Universitária "Zeferino Vaz", 13083-860 - Campinas - SP
Brazil,
E-mail: ana.carolina@fem.unicamp.br

ABSTRACT

Even though most part of the planet is covered by water, many regions experiences situation of severe draught. Solar still devices presents as a solution to scarcity of water in hot climate regions, where electricity does not reach. These devices are very simple and present ability of converting available saline or low quality water into potable water. In this work, multi-physics of an inclined square solar still device are numerically studied through finite volume method. The phenomenon of double-diffusion natural convection is considered for problem modeling. Velocities, temperature and concentration fields are obtained when Rayleigh number is varied from 10^4 to 10^7. Solar still capacity is analyzed through condensation rate parameter, for the mentioned Rayleigh number range.

INTRODUCTION

Water supply has become a major difficulty in the world due to population growth, rise in living standards, and industry development [1]. Today, there are about 10.000 desalination plants around the world, where Saudi Arabia and United States stand as the greatest users of this technology [2]. Desalination, however, has proved to be a competitive technology that can be used in small scale, especially in isolated communities in situation of vulnerability that experience draught [3].

The process of desalination through distillation is the oldest process to separate water from salts, and is based on the fact that only water is volatile. Pure water evaporates out of saline water by heat transfer and condenses by heat removal [4]. Pure natural convection is a phenomenon that takes place in many engineering processes, thus many academic studies have been performed in this theme [5,6,7]. Binary natural convection studies due to thermal and solutal gradients, however, are harder to find.

A numerical study considering double-diffusion in a closed square cavity filled with air and pollutants was performed by Béghein et al. [8], comparing the effects of thermal and solutal buoyancy forces, through Nusselt and Sherwood numbers. It was found that, for a solute diffusively dominated flow, the concentration boundary layer is rather thick, while in a thermal diffusively dominated flow the concentration boundary layer is thinner. Numerical and experimental investigations in double-natural convection [8,9] show that the direction of the fluid may be reversed if the buoyance parameter (expansion coefficient) is changed from negative to positive.

NOMENCLATURE

C^*	[-]	Dimensionless species concentration
g	[m/s^2]	Gravity acceleration
H	[m]	Cavity height and length
h_{cw}	[W/mK]	Convective heat transfer coefficient
h_{fg}	[J/kg]	Latent heat of vaporization
k	[W/m.K]	Thermal conductivity
c_p	[J/kg.K]	Specific heat
T	[K]	Temperature
D_v	[m^2/s]	Species diffusivity
C	[kmol/m^3]	Species molar concentration
Le	[-]	Lewis number
M	[kg/kmol]	Molecular weight
$\dot{m}_v$	[kg/mh]	Water condensation rate
N	[-]	Buoyancy ratio
Nu	[-]	Nusselt number
p	[Pa]	Pressure
Pr	[-]	Prandtl number
q_e	[W/m]	Evaporation rate
Ra	[-]	Rayleigh
Sh	[-]	Sherwood number
t	[s]	Time
T^*	[-]	Dimensionless temperature
u^*,v^*	[-]	Dimensionless velocities
u,v	[m/s]	Dimensional velocities
x^*,y^*	[-]	Dimensionless local coordinates
x,y	[m]	Dimensional local coordinates

Special characters

θ	[^{o}]	Tilt angle
$\in$	[-]	Dimensionless temperature parameter
ν	[m^2/s]	Kinematic viscosity
β_S	[m^3/kmol]	Solutal expansion coefficient
β_T	[1/K]	Thermal expansion coefficient
α	[m^2/s]	Thermal diffusivity
μ	[Pa.s]	Dynamic viscosity
ρ	[kg/m^3]	Density
$\Re$	[J/kmolK]	Universal gas constant

Subscripts

a	Air
c	Cold
h	Hot
v	Vapor

An important parameter for solar still design and performance is the vapor flow rate leaving the saline water, at the hot surface. Jabrallah et al. [10], who have numerically studied heat and mass transfer in a solar distillation system, concluded that the distillation cell performance could be improved by increasing heat on the hot surface or raising the temperature of incoming water. Chenoweth and Paolucci [11], however, points out that for large temperature differences, the flow becomes very sensitive to properties variations and Boussinesq approximation must be used carefully. Thus, there is a risk that Boussinesq limits are extrapolated. Le Quéré et al. [7] infers that for larger temperature differences, the flow becomes compressible and the dependence to its properties becomes larger. In his work, Boussinesq approximation was not used. Thermo-physical properties (viscosity and thermal conductivity) were considered variables through the Sutherland law. Alvarado-Juárez et al. [12] simulated Nusselt number related to the inclination angle of the cavity. They found that the Nusselt increased as the inclination angle increased.

This paper aims to numerically investigate a simple solar still, modelling the device as an inclined cavity where double-diffusive natural convection phenomenon takes place. With the results, condensation rate was estimated and its capacity evaluated. Temperature difference is considered low, thus, a Boussinesq is considered and thermophysical properties variation is small enough to be disregarded.

ANALYSIS

The considered domain of the solar still in analysis is a two-dimensional square cavity, as shown in Figure 1. Vertical walls are adiabatic and impermeable. Upper and bottom walls are at different levels of temperature, so fluid motion is generated. The temperature of bottom wall is slightly higher than upper wall. At the bottom, a thin liquid layer is present and vapor is considered to form at saturated state. Upper wall consists of a glass cover, which is at lower temperature. At lower temperature wall, the new species (vapor) condenses out of the mixture inside the cavity.

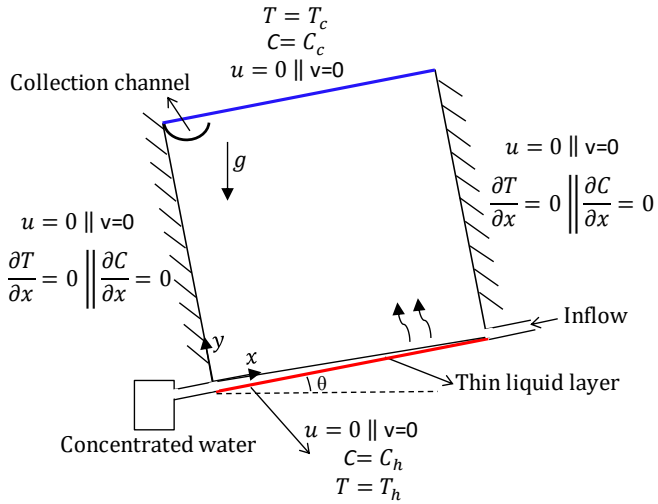

Figure 1 Model for binary natural convection of an inclined solar still

The representation of fluid dynamics, heat and mass transfer in the cavity is done considering conservative equations. These equations were expressed in terms of differentials. The variables are the same as the pure convection problems, adding an additional quantity: concentration of vapor. Considering the local coordinate system, the continuity equation is:

$$\frac{\partial \rho}{\partial t} + \frac{\partial (\rho u)}{\partial x} + \frac{\partial (\rho v)}{\partial y} = 0 \tag{1}$$

Momentum equation are:

$$-\frac{\partial p}{\partial x} + \mu\left(\frac{\partial^2 u}{\partial x^2} + \frac{\partial^2 u}{\partial y^2}\right) + \left(\rho - \rho_{ref}\right) g sin(\theta) = \frac{\partial (u\rho)}{\partial t} + \frac{\partial (\rho u \cdot u)}{\partial x} + \frac{\partial (\rho v \cdot u)}{\partial y} \tag{2}$$

$$-\frac{\partial p}{\partial y} + \mu\left(\frac{\partial^2 v}{\partial x^2} + \frac{\partial^2 v}{\partial y^2}\right) + \left(\rho - \rho_{ref}\right) g \cos(\theta) = \frac{\partial (v\rho)}{\partial t} + \frac{\partial (\rho u \cdot v)}{\partial x} + \frac{\partial (\rho v \cdot v)}{\partial y} \tag{3}$$

Energy equation is:

$$\frac{k}{c_p}\left(\frac{\partial^2 T}{\partial x^2} + \frac{\partial^2 T}{\partial y^2}\right) = \frac{\partial (\rho T)}{\partial t} + \frac{\partial (\rho u \cdot T)}{\partial x} + \frac{\partial (\rho v \cdot T)}{\partial y} \tag{4}$$

Species concentration equation is:

$$D_v\left(\frac{\partial^2 C_v}{\partial x^2} + \frac{\partial^2 C_v}{\partial y^2}\right) = \frac{\partial (C_v)}{\partial t} + \frac{\partial (u \cdot C_v)}{\partial x} + \frac{\partial (v \cdot C_v)}{\partial y} \tag{5}$$

In this analysis, the thermal viscous dissipation has been neglected, as well as heat generation and chemical reactions. The fluid is considered to be Newtonian and the regime laminar. The buoyance term is evaluated by Boussinesq approximation:

$$\left(\rho - \rho_{ref}\right) = \rho\beta_T\left(T_{ref} - T\right) + \rho\beta_S\left(C_{ref} - C\right) \tag{6}$$

The conservative equations variables are non-dimensionalized according to the local coordinate system:

$$T^* = \frac{T - T_c}{T_h - T_c}, x^* = \frac{x}{H}, y^* = \frac{y}{H}, u^* = \frac{uH}{\alpha}, v^* = \frac{vH}{\alpha}, C^* = \frac{C - C_c}{C_h - C_c} \tag{7}$$

The temperature difference between hot and cold wall may be defined by the non-dimensional parameter:

$$\in = \left(T_h - T_c\right) / \left(T_h + T_c\right) \tag{8}$$

Thermal and solutal expansion coefficients are respectively given by [10]:

$$\beta_T = -\frac{1}{\rho}\left(\frac{\partial \rho}{\partial T}\right)_p = \frac{1}{T_{ref}} \qquad (9)$$

$$\beta_S = -\frac{1}{\rho}\left(\frac{\partial \rho}{\partial C}\right)_{p,T} = \frac{M_a - M_v}{C_{ref} M_v + C_a M_a}$$

Thermal Rayleigh number is defined as:

$$Ra_T = \frac{g\beta_T (T_h - T_c) H^3}{\nu\alpha} \qquad (10)$$

Solutal Rayleigh number is defined as:

$$Ra_S = \frac{g\beta_S (C_h - C_c) H^3}{\nu D_v} \qquad (11)$$

Prandtl and Lewis number:

$$\mathrm{Pr} = \frac{\nu}{\alpha} \text{ and } Le = \frac{\alpha}{D_v} \qquad (12)$$

The reference temperature (T_{ref}) and concentration (C_{ref}) are (T_h + T_c)/2 and (C_h + C_c)/2 respectively. The local Nusselt and Sherwood number along a horizontal axis are evaluated from the expressions:

$$Nu = uT^* - \frac{\partial T^*}{\partial y^*} \qquad (13)$$

$$Sh = Le\left(uC^* - \frac{1}{Le}\frac{\partial C^*}{\partial y^*}\right) \qquad (14)$$

The ratio between solutal and thermal buoyancy forces are determined by the dimensionless parameter:

$$N = \frac{\beta_S \Delta C}{\beta_T \Delta T} \qquad (15)$$

For gas stream-liquid interface experiencing evaporation, Raoult´s Law infers that the partial pressure of the vapor at the water-air interface corresponds to saturated conditions at the interface temperature [2], thus p_h=p_{sat}(T_h). At the cold wall where condensation occurs, p_c=p_{sat}(T_c). The evaporation per hour per meter square is shown and demonstrated by Tiwari [13]:

$$q_e = 0.0162 h_{cw}(p_h - p_c) \qquad (16)$$

The convective heat transfer coefficient from water surface to glass (h_{cw}):

$$Nu = \frac{h_{cw} H}{k} \qquad (17)$$

The total hourly condensation rate (water yield) per area can be determined by the equation:

$$\dot{m}_w = \frac{q_e}{h_{fg}} \times 3600 \qquad (18)$$

Boundary Conditions

Natural convection is induced due to temperature difference, in a cavity of dimension $0 \le x \le H$ and $0 \le y \le H$. The tilt angle is θ=25°. The non-dimensional temperature difference is defined to be ϵ=0.02 and T_{ref} = 300 K.

The boundary conditions of the defined problem are:

$$u(0,y) = u(H,y) = u(x,0) = u(x,H) = 0 \qquad (19)$$

$$v(0,y) = v(H,y) = v(x,0) = v(x,H) = 0 \qquad (20)$$

$$T(x,0) = T_h = T_{ref}(1+\in) \qquad (21)$$

$$T(x,H) = T_c = T_{ref}(1-\in) \qquad (22)$$

$$\frac{\partial T(0,y)}{\partial y} = \frac{\partial T(H,y)}{\partial y} = \frac{\partial C(0,y)}{\partial y} = \frac{\partial C(H,y)}{\partial y} = 0 \qquad (23)$$

The air and water vapor in the cavity is considered to be an ideal gas. Concentrations at hot and cold surface are determined by the state equation for an ideal gas. Thus, for the surfaces:

$$C_v(x,0) = \frac{p_{sat}(T_h)}{\Re T_h} \qquad (24)$$

$$C_v(x,H) = \frac{p_{sat}(T_c)}{\Re T_c} \qquad (25)$$

The domain contains air and water vapor, thus properties are assumed to be constant and at the reference temperature:

$$k = 2.63\times10^{-2} W/mK$$
$$c_p = 1.007\times10^{3} J/kgK \qquad (26)$$
$$\rho = 1.1614 kg/m^3$$

Other parameters are considered:

$$\mathrm{Pr} = 0.71$$
$$D_v = 0.26\times10^{-4} m^2/s \qquad (27)$$

NUMERICAL METHOD

The numerical solution method initiates with conservative equations (1-5) discretization, utilizing the finite volume method. The resolution of discretized equations is performed by SIMPLE algorithm (abbreviation for Semi-Implicit Method for Pressure-Linked Equations), as presented by Patankar [14]. This procedure consists of correcting velocities iteratively, through the momentum and continuity equations. Other quantities, such as temperatures and concentrations, are obtained by energy and species conservation equations, also through iterative method. False transient formulation and fully implicit scheme for time discretization is utilized [14]. Scalar variables are calculated in a 60x60 main grid while velocities components are calculated in a staggered grid. Both grids are non-uniform and meet a hyperbolic tangent function, as presented by Sengupta [15], ensuring thinner spacing close to the walls.

The approximation of convective term present in conservative equation is done by upwind scheme while the

diffusive term is approximated by central difference. Under-relaxation was used to improve convergence of the algorithm. The convergence is reached when the residue of conservation equations is less than 10^{-10}.

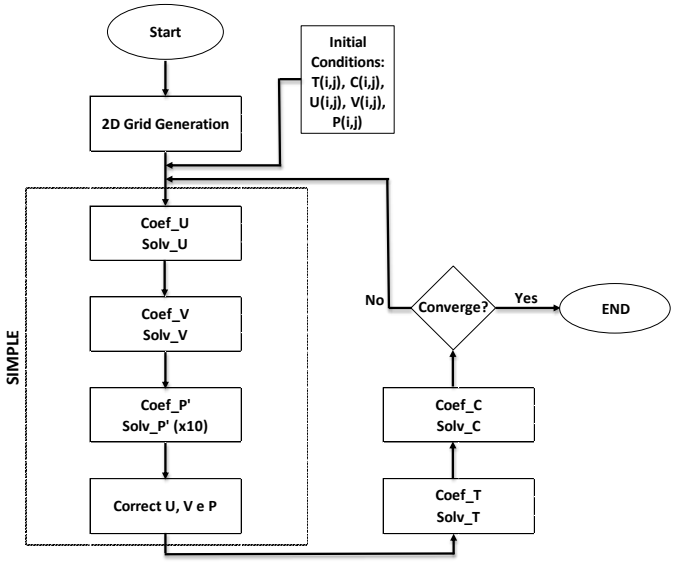

Figure 2 Numerical method for binary natural convection of a solar still

Validation of Numerical Models

The validation of the numerical code was done for the heat and mass transfer in a square cavity situation. The results were compared to the benchmark work published by Béghein et al. [8] and to the paper published by Alvarado-Juárez et al. [16]. Both comparisons were performed to a differentially heated square cavity with mass concentration difference between vertical walls.

A quantitative verification was performed comparing the average Nusselt number along the hot vertical for different buoyance ratios (from -0.01 to 5.0) and fixed thermal Rayleigh of $Ra_T=10^7$. This verification can be found on Table 1. The maximum error found was 1.62% for N=-5.0 corresponding to the comparison with Alvarado-Juárez et al. [16].

A qualitative verification was done for thermosolutal convection considering $Ra_T=10^4$ and $Ra_S=10^4$ (Figure 3). Both qualitative and quantitative verification considered Pr=0.71 and Le=1.0.

Table 1 Average Nusselt numbers (along a vertical axis) for $Ra_T=10^7$ and N varing from -0.01 to -5

N	-0.01	-0.2	-0.8	-1.5	-5.0
Ra_S	10^5	$2x10^6$	$8x10^6$	$1.5x10^7$	$5x10^7$
Béghein et al. [8]	16.4	15.5	10.6	13.6	23.7
Alvarado-Juárez et al. [14]	16.53	15.61	10.68	13.74	24.05
Present work	16.36	15.45	10.61	13.62	23.66

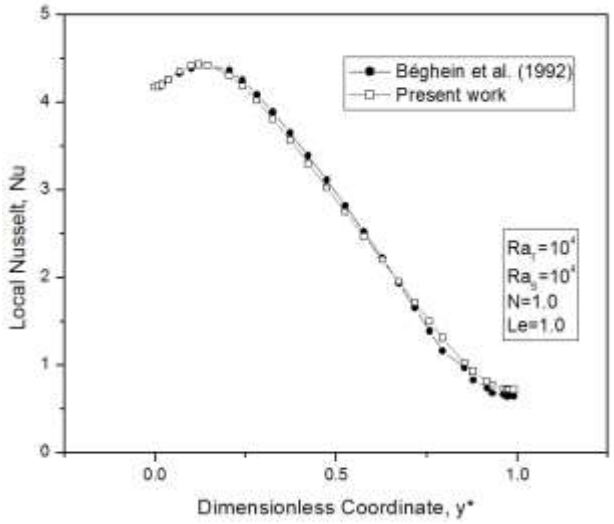

Figure 3 Comparison of local Nusselt number along the hot wall of an enclosed cavity.

RESULTS AND DISCUSSION

Numerical solutions for heat and mass transfer simulation inside a solar still cavity were obtained. In order of keeping the flow at laminar regime, computation was performed for thermal Rayleigh number between 10^3 and 10^6. The temperature difference between hot and cold wall is low, thus properties variations may be disregarded and the mathematical model is appropriate. Top and bottom walls also experience different water vapor concentration, based on saturation conditions of the water and the temperature of the walls.

Figure 4 illustrates temperature isolines inside the solar still cavity for the mentioned thermal Rayleigh range. As Rayleigh number increases from 10^3 and 10^6, temperature isolines tend to approximate and the thermal boundary-layer become thinner. The fluid in the core region experiments smaller gradients of temperature, and as Rayleigh becomes higher, variations of temperature in the core becomes even smaller.

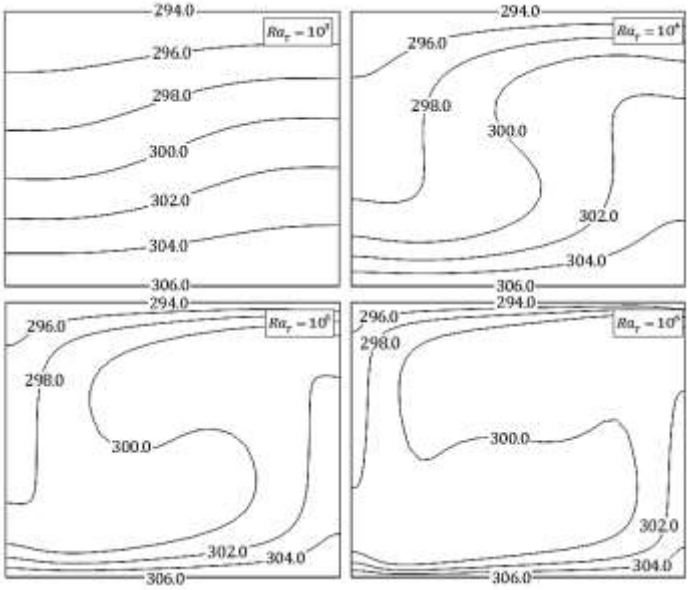

Figure 4 Temperature isolines for $Ra_T=10^3$ to 10^6 and θ=25°

Streamlines inside the still cavity are represented in Figure 5 for different Rayleigh numbers. These lines also tend to approximate as thermal buoyancy forces becomes higher and present smaller gradient of velocities in the core region. Streamwise vortices form, representing the first changes in the flow boundary layer and become larger as Rayleigh increases. Temperature (Figure 4) and concentration (Figure 6) isolines present similar behavior for Rayleigh number increase. Concentration isolines tend to stack close to the walls. The approximation of these lines occurs saliently at the left side of the bottom wall, indicating that the concentration of water vapor is higher in that area. As Rayleigh increases concentration of water vapor boundary layer becomes thinner and concentration of water vapor becomes less diffused. Core region is filled with a homogeneous mixture.

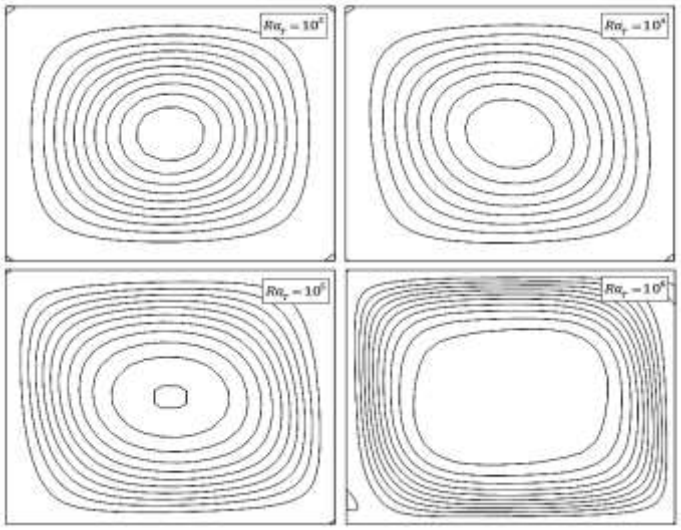

Figure 5 Streamlines for $Ra_T=10^3$ to 10^6 and $\theta=25°$

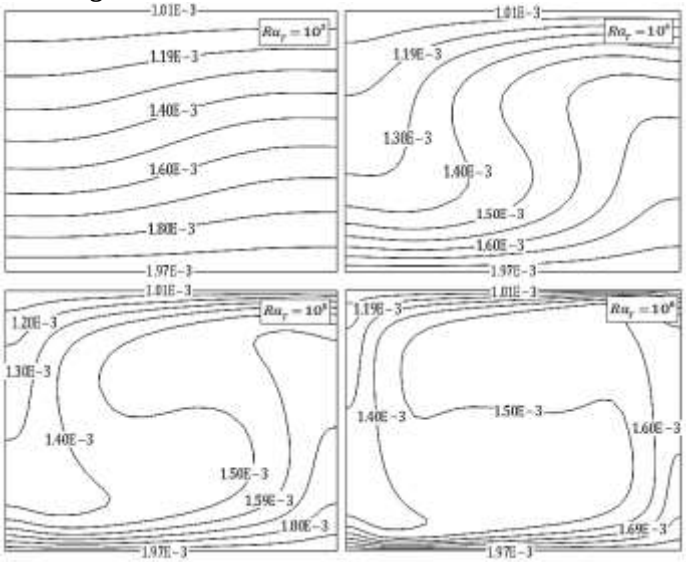

Figure 6 Concentration isolines for $Ra_T=10^3$ to 10^6 and $\theta=25°$

Vapor formation occurs prominently at the higher temperature wall, thus higher temperature and concentration find at the same side of domain. Since buoyancy parameters are considered to be positive, thermal and solutal buoyancy forces aid each other (flow the same direction). The flow in the cavity is thermal dominated (thermal Rayleigh is higher than solutal). The temperature and concentration difference between hot and cold wall tend to induce the convection pattern and, since the cavity is inclined, the flow in the cavity moves counterclockwise. This behavior can be noticed through the isolines presented in this work.

Local Nusselt and Sherwood numbers were obtained and are represented in Figures 7 and 8 along the hot wall. These lines tend to overlap for Le=1.0 (same binary and thermal diffusivity values). For the present work Le=0.87, thus Sherwood values are slightly lower than Nusselt, as can be noticed in the figures. Both Nusselt and Sherwood increase with Rayleigh and experience a peak at the left side of the hot wall because the gradient of temperatures and concentration are respectively higher in that area.

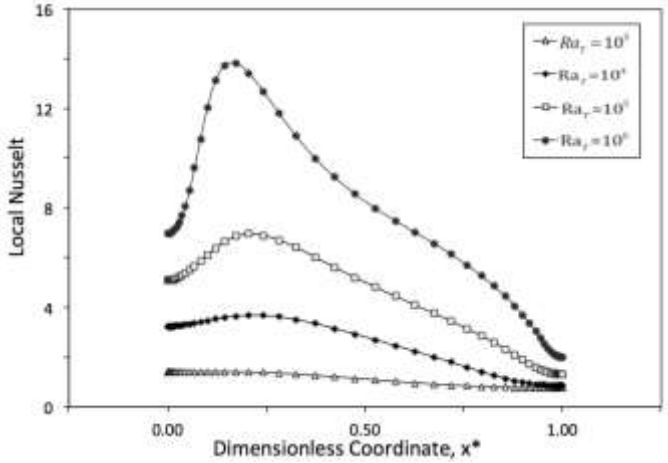

Figure 7 Local Nusselt along the hot wall of solar still cavity for $Ra_T=10^3$ to 10^6 and $\theta=25°$

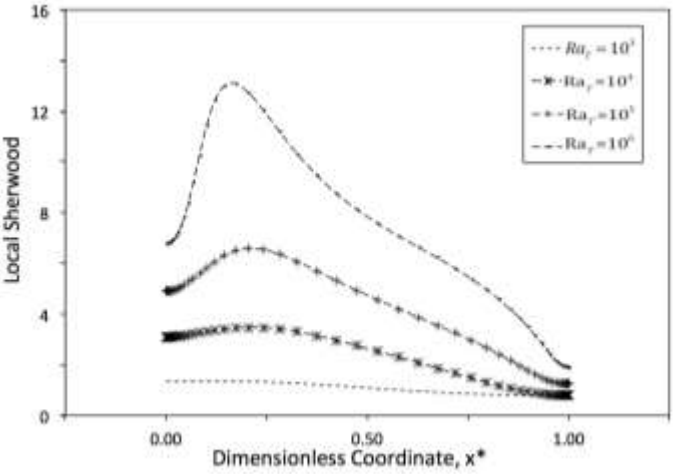

Figure 8 Local Sherwood along the hot wall of solar still cavity for $Ra_T=10^3$ to 10^6 and $\theta=25°$

Average Nusselt, Sherwood and local condensation rate along a horizontal axis can be found in Table 2. For for higher average Nusselt, condensation rate tends to increase. Thus, the highest value for condensation rate was experienced for Rayleigh equals to 10^6. Evaluation for higher Rayleigh numbers

could be possible, however, boundary layer would begin to become turbulent and this model would not be appropriate.

Table 2 Average Nusselt, Sherwood and condensation rate along a horizontal axis for $Ra_T=10^3$ to 10^6 and $\theta=25°$

Ra_T	10^3	10^4	10^5	10^6
Nusselt	1.1	2.54	4.61	8.15
Sherwood	1.08	2.39	4.37	7.73
Condensation Rate (kg/mh)	0.0017	0.0040	0.0073	0.0129

Solar still local condensation rate was obtained calculating the convective heat transfer coefficient from water surface to the glass, which could be calculated through the dimensionless parameter local Nusselt. Local values for condensation related to the dimensionless coordinate x are shown in Figure 9. The similarity in curves behaviour between Nusselt and local condensation rate can be noticed. Thus, local condensation rate tends to increase with Rayleigh number. However, for high Rayleigh numbers, a high temperature and concentration gradients are present at the left side of the wall, thus a great peak of condensation is experienced in this region. The higher the Rayleigh, the higher the peak is.

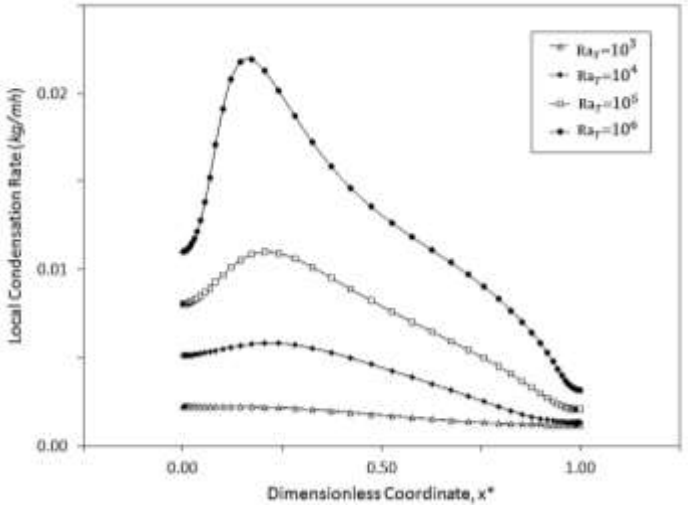

Figure 9 Local condensation rate along a horizontal axis for $Ra_T=10^3$ to 10^6 and $\theta=25°$

CONCLUSION

Conservation of mass, momentum, energy and concentration of a solar still cavity were numerically studied for laminar convection considering the Rayleigh range between 10^3 and 10^6. Higher Rayleigh numbers results in changes in the fluid dynamics inside the solar still, causing changing solar still performance. As Rayleigh number increase, temperature, concentration and velocities isolines tend to approximate in direction of the walls, thus these gradients become higher. Higher Nusselt and Sherwood numbers exist at the walls. At the left side of the hot wall, the greatest gradients of temperature and concentration can be found. Consequently, high Nusselt peaks exists there.

Simulations shown that for higher Rayleigh numbers, higher condensation rates occurs. Nusselt and local condensation rate profiles are similar, therefore a peak of condensation rate exist in the regions of higher Nusselt number. Thus, a higher gradient of temperature influence the condensation production. The highest condensation rate happened when Rayleigh was 10^6.

REFERENCES

[1] Xiao G., Wang X., Ni M., Wang F., Zhu W., Luo Z., and Cen K., A review on solar stills for brine desalination, *Applied Energy*, Vol. 103, 2013, pp. 642-652

[2] Çengel Y., and Boles, Thermodynamics: an engineering approach, McGraw-Hill Education, 2015

[3] Banat F., and Jwaied N., Economic evaluation of desalination by small-scale autonomous solar-powered membrane distillation units, *Desalination*, Vol. 220, 2008, pp. 566-573

[4] Cerci Y., The minimum work requirement for distillation process, *Exergy, an International Journal*, Vol. 2, 2002, pp. 15-23

[5] Le Quéré P., Accurate solutions to the square differentially heated cavity at high rayleigh number, *Computers Fluids*, Vol. 20, 1991, pp. 29-41

[6] Vahl Davis G., Natural convection of air in a square cavity: a bench mark numerical solution, *International Journal for Numerical Methods in Fluid*, Vol. 3, 1983, pp. 249-264

[7] Le Quéré P., Weisman C., Paillère H., Vierendeels J., Dick E., Becker R., Braack M., and Locke J., Modeling of natural convection flows with large temperature differences: a benchmark problem for low mach number solvers. part 1. reference solutions, *ESAIM: Mathematical Modeling and Numerical Analysis*, 2005, pp. 609-616

[8] Béghein C., Haghighat F., and Allard F., Numerical study of double-diffusive natural convection in a square cavity, *International Journal of Heat and Mass Transfer*, Vol. 35, 1992, pp. 833-846

[9] Weaver J. A., and Viskanta R., Natural convection in binary gases driven by combined horizontal thermal and vertical solutal gradients, *Experimental Thermal and Fluid Science*, Vol. 5, 1992, pp. 57-68

[10] Jabrallah S. B., Belghith A., and Corriou J. P., Etude des transfer couplés de matière et de chaleur dans une cavité rectangulaire: application à une cellule de distillation, *International Journal of Heat and Mass Transfer*, Vol. 45, 2002, pp. 891-904

[11] Chenoweth D. R., and Paolucci S., Natural convection in an enclosed vertical air layer with large horizontal temperature, *Journal of Fluid Mechanics*, Vol. 169, 1986, pp. 173-210

[12] Alvarado-Juárez R., Álvarez G., Xamán J., and Hernández-López, Numerical study of conjugate heat and mass transfer in a solar still device, *Desalination*, Vol. 325, 2013, pp. 84-94

[13] Tiwari G. N., Tiwari A., and Shyam, Handbook of solar energy: theory, analysis and applications, Springer, 2016

[14] Patankar S., Numerical heat transfer and fluid flow, *CRC Press*, 1980

[15] Sengupta T. K., Bhaumik S., and Shameen U., A new compact difference scheme for second derivative in non-uniform grid expressed in self-adjoint form, *Journal of Computational Physics*, Vol. 230, 2011, pp. 1822-1848

[16] Alvarado-Juárez R., Álvarez G., Xamán J., and Hernández-López I., Numerical study of conjugate heat and mass transfer in a solar still device, *Desalination*, Vol. 325, 2013, pp. 84-94